Supporting information

Design and synthesis of functionalized defective MOFs for catalytic conversion of CO_2 to cyclic carbonates under green conditions

S1 Reagents

Hafnium chloride ($HfCl_4$), N, N-dimethylformamide (DMF), acetone, toluene, N-methylpyrrolidone (NMP), deionized water (DI), formic acid (HCOOH), acetic acid (HAc), benzoic acid (BA), trifluoroacetic acid (TFA), ethanol (EA), epichlorohydrin (ECH), epibromohydrin (EBH), styrene oxide (SO), chloroform-d ($CDCl_3$), dimethyl sulfoxide d_6 (DMSO), dimethyl carbonate (DMC), hydrochloric acid (HCl), sodium hydroxide (NaOH), 2-bromoterephthalic acid (H_2BDC-Br), imidazole (IM), anhydrous potassium carbonate (K_2CO_3), anhydrous copper sulfate ($CuSO_4$). All the reagents are of analytical grade and used without further purification.

S2 Synthesis of 2-(imidazole-1-yl) terephthalic acid[1-7].

A mixture of K_2CO_3 (1.9340 g, 0.014 mol), 2-bromoterephthalic acid (1.2250 g, 0.005 mol), imidazole (1.7100 g, 0.025 mol), $CuSO_4$ (0.0500 g, 0.2 mmol) was sufficiently ground in an agate mortar. Then, the mixture was transferred into a 100 mL Teflon lined autoclave, which was sealed and heated at 200°C for 10 h. After cooling the reaction system to room temperature, the reaction mixture was dissolved in 60 mL water, and then filtered off. The green filtrate was adjusted with 6 M dilute hydrochloric acid to pH 2.0-3.0 and filtered to obtain yellow filtrate. Recrystallization from dilute

hydrochloric acid yielded colourless rod crystals of $H_2BDC{\cdot}IM{\cdot}HCl{\cdot}H_2O$.

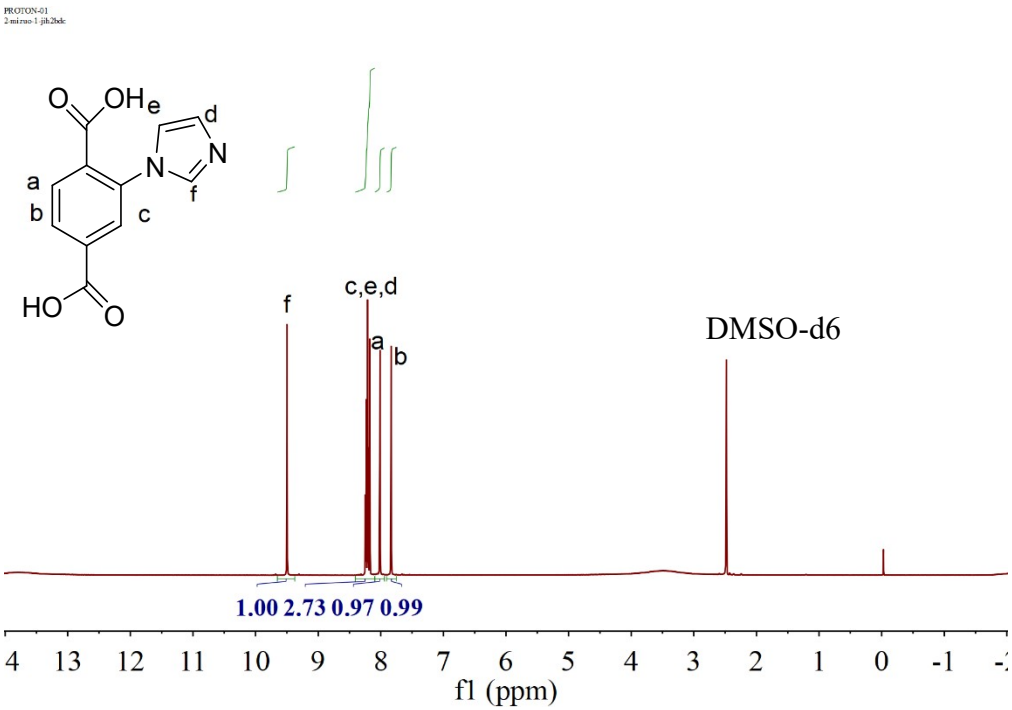

Fig. S1 ^1H NMR of $H_2BDC{\cdot}IM{\cdot}HCl{\cdot}H_2O$ in DMSO-d6**.**

Table S1 Elemental analysis of $H_2BDC{\cdot}IM{\cdot}HCl{\cdot}H_2O$.

Elements	C [%]	N [%]	H [%]
$H_2BDC{\cdot}IM{\cdot}HCl{\cdot}H_2O$	45.73	9.57	3.831

The analysis results of the C, N, H elements (Table S1) are basically consistent with the theoretical values, which are C: 45.72%, N: 9.70%, H: 3.810% including H in HCl molecule and crystal water.

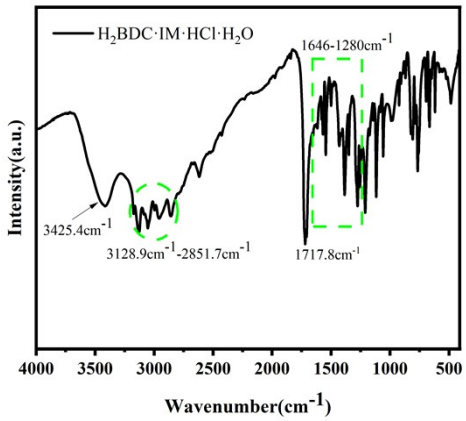

Fig. S2 FT-IR of $H_2BDC{\cdot}IM{\cdot}HCl{\cdot}H_2O$.

As shown in Fig. S2, the absorption peak at 3425.4cm^{-1} corresponds to the water-binding -OH in the ligand, the C=C expansion vibration peak on the benzene ring appears at 3128.9-2851.7 cm^{-1}, the skeleton vibration peak of the benzene ring is in the range of 1646~1280 cm^{-1}, and the absorption peak of the carbonyl group is at 1717.8 cm^{-1}. The absorption vibration peak of imidazole appeared between 1053 and 1202 cm^{-1}.

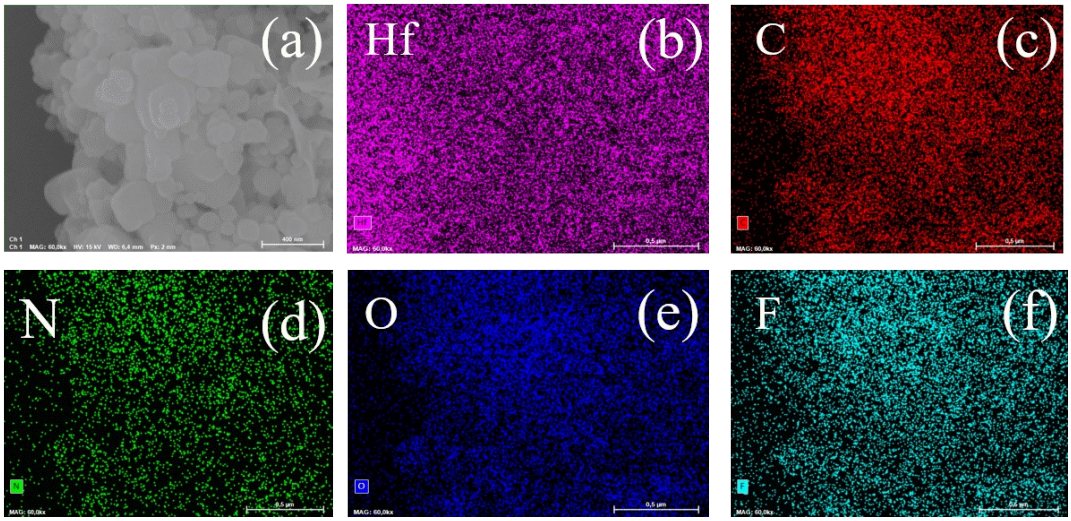

Fig. S3 EDS-mapping of HUIN MOFs.

S3 Calculation of activation energy[8]

In this paper, a rough calculation of the activation energy is performed. As known, activation energy is the energy required for a molecule to change from its normal state to an active state that is prone to chemical reactions. The activation energy is the difference between the average energy of the activated molecule and that of the reactant molecule. It is an energy barrier that needs to be overcome for a chemical reaction to occur. The general rate equation for the cycloaddition reaction can be described as Eq. (1), where k is the rate constant and *[ECH]*, *[CO_2]*, *[CAT]* are the concentrations of ECH, CO_2 and catalyst, respectively; a, b and c are the orders of the reaction. The concentration of the catalysts remained constant during each experiment, and that of CO_2 remained steady throughout the reaction, and can be assumed to be constant due to continuous supplement. Therefore, Eq. (1) was simplified as Eq. (2), and $ka = k\cdot[CO_2]^{b}\cdot[CAT]^{c}$. Assuming pseudo-first-order dependence of the reaction on epoxide

concentration i.e., a = 1 and by combining Eqs. (2) and (5), the rate of reaction can be given as Eq. (6). By integrating Eq. (6), the obtained Eq. (7) can be used to determine the order of reaction with respect to *[ECH]*. The reaction rate constant (*ka*) was calculated from the gradient of ln[1/(1-**α**)] vs. reaction time (t). And the linearity of all these plots indicates the first-order reaction kinetic for CO_2 cycloaddition (**α** representing the ECH conversion). The formulas are as follows**:**

Arrhenius equation **:** $Ka = A \cdot exp(-\frac{Ea}{RT}) \longrightarrow lnKa = -\frac{Ea}{R} \cdot \frac{1}{T} + lnA$

Rate = $k \cdot [ECH]^a \cdot [CO_2]^b \cdot [CAT]^c$ (1)

Rate = $ka \cdot [ECH]^a$ (2)

Where $ka = k \cdot [CO_2]^b \cdot [CAT]^c$ (3)

$\ln ka = \ln k + b \cdot \ln[CO_2] + c \cdot \ln[CAT]$ (4)

Rate = $-d[ECH]/dt$ (5)

$-d[ECH]/dt = ka \cdot [ECH]$ (6)

$-\ln[ECH] = ka \cdot t$ (7)

Table S2 HUI_4 MOF catalyzes the conversion of CO_2 and ECH to CPC.

t/h	4	6	8	10	12
ECH conversion (**α**)/%	13.58	23.90	31.30	49.00	45.46
ln(1/(1-**α**))	0.1460	0.2731	0.3754	0.6733	0.6062

Table S3 HUIN MOFs catalyzes the conversion of CO_2 and ECH to CPC**.**

t/h	4	6	8	10	12
ECH conversion (**α**)/%	53.55	55.95	64.29	81.64	79.65
ln(1/(1-**α**))	0.7668	0.8198	1.0297	1.6950	1.5921

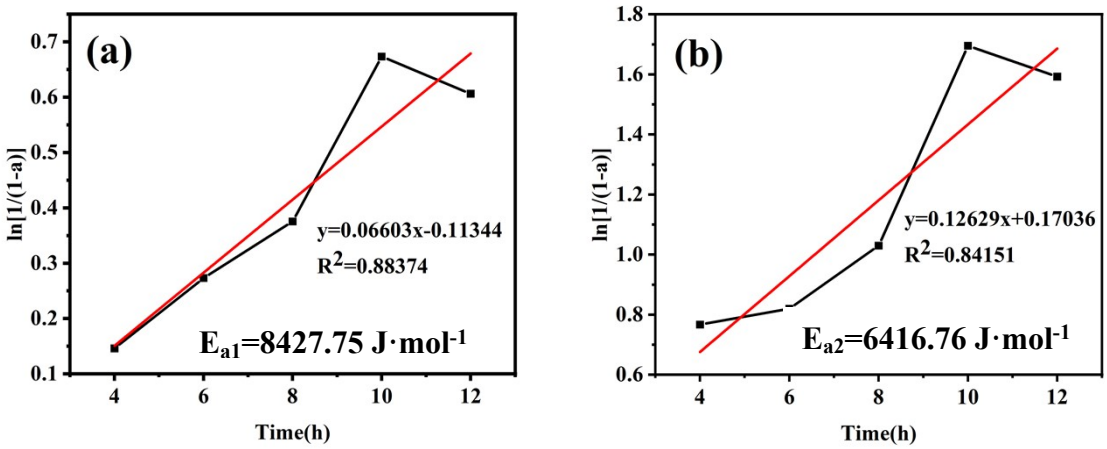

Fig. S4 ln[1/(1-α)] linear fitting on t for HUI_4 (a) and HUIN (b), respectively.

In the catalytic reaction, the conversion temperature is constant with T=373K, so E_{a1} = 8427.75 J·mol^{-1}, E_{a2} = 6416.76 J·mol^{-1} are calculated with E_{a1} ＞ E_{a2}.

It is proved that HUIN MOF has lower activation energy than HUI_4 MOF, and thus displays higher ECH conversion rate.

Table S4 Comparison of the catalytic performance of HUIN with those of previously reported MOFs for cycloaddition of CO_2 with ECH.

Entry	Catalyst	Cocatalyst	Time (h)	Temperature (℃)	Pressure （MPa）	Yield (%)	Ref.
1	NU-912(Hf)−I	-	6	55	1	＜5	9
2	FJI-H6	TBAB	60	25	1	52.6	10
3	PCP-33(Mn)	TBAB	12	80	1	72.27	11

4	HUIN	-	10	100	0.1	76.12	This Work

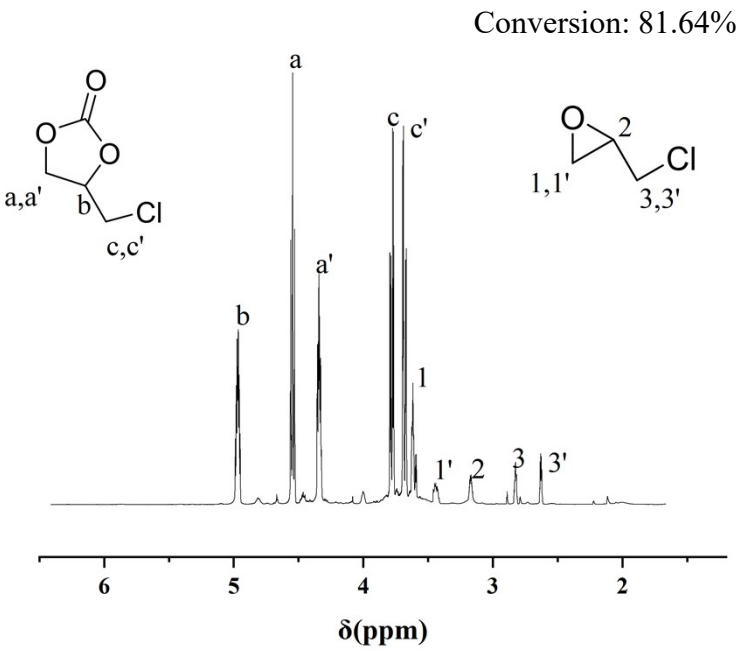

Fig. S5 [1]H NMR of ECH conversion to 4-(chloromethyl)-1,3-dioxolan 2-one.

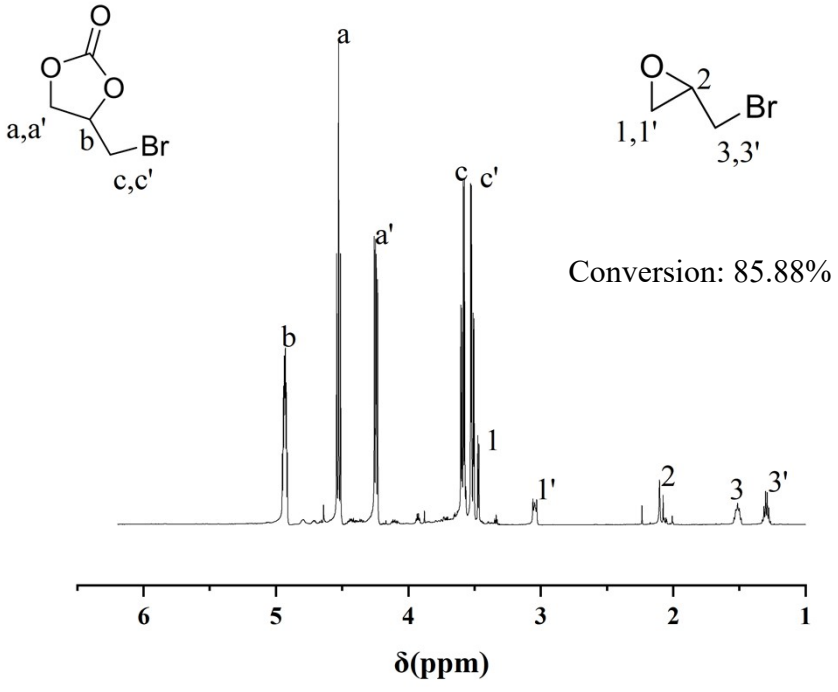

Fig. S6 ^{1}H NMR of EBH conversion to 4-(bromomethyl)-1,3-dioxolan-2-one.

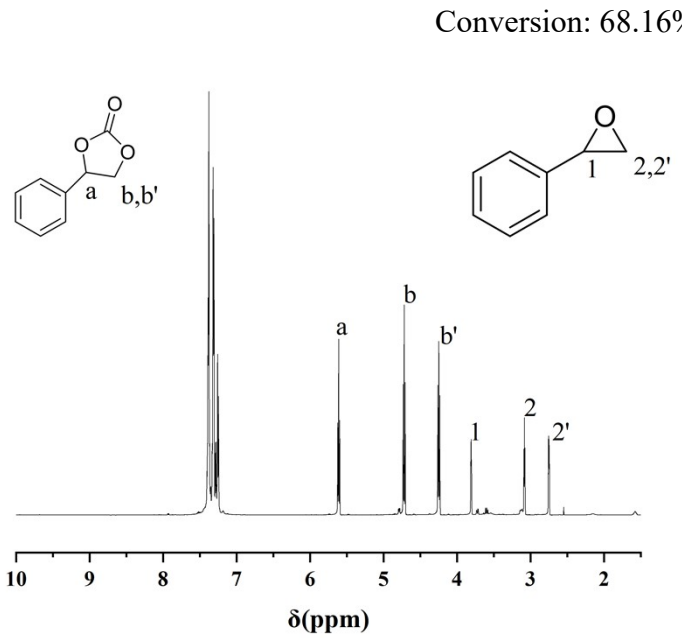

Fig. S7 ^{1}H NMR of SO conversion to 4-(phenyl)-1,3- dioxolan-2-one.

Reference

1. K. H. Cui, S. Y. Yao, H. Q. Li, Y. T. Li, H. P. Zhao, C. J. Jiang and Y. Q. Tian, CrystEngComm, 2011, 13, 3432.
2. S. Gulati, S. Vijayan, S. Kumar, B. Harikumar, M. Trivedi, R. S. Varma and R. S. Varma, Coord. Chem. Rev., 2023, 474, 46.
3. F. F. Li, Y. Chen, A. J. Gao, W. J. Tong, C. C. Ji, Y. Cheng and Y. H. Zhou, New J. Chem., 2022, 46, 18418-18425.
4. X. Y. Li, Y. Z. Li, L. N. Ma, L. Hou, C. Z. He, Y. Y. Wang and Z. H. Zhu, J. Mater. Chem. A, 2020, 8, 5227-5233.
5. J. Liang, R. P. Chen, X. Y. Wang, T. T. Liu, X. S. Wang, Y. B. Huang and R. Cao, Chem. Sci., 2017, 8, 1570-1575.
6. H. Molavi, F. A. Joukani and A. Shojaei, Ind. Eng. Chem. Res., 2018, 57, 7030-7039.
7. X. Zhang, Y. L. Jiang and H. H. Fei, Chem. Commun., 2019, 55, 11928-11931.
8. A. Rehman, V. C. Eze, M. Resul and A. Harvey, J. Energy Chem., 2019, 37, 35-

42.

9. L. L. Wang, W. Z. Qiao, H. Liu, S. W. Li, J. Wu and H. W. Hou, Inorg. Chem., 2023, DOI: 10.1021/acs.inorgchem.2c04078, 10.
10. M. Feng, X. Zhou, X. R. Wang, P. P. Zhou, J. Y. Wang, Z. Y. Cheng and D. M. Wang, ACS Appl. Mater. Interfaces, 2023, 15, 11837-11844.
11. J. Zheng, M. Wu, F. Jiang, W. Su and M. Hong, Chem Sci, 2015, 6, 3466-3470.